厚生労働科学研究費補助金

循環器疾患等生活習慣病対策総合研究事業

冠動脈不安定粥腫の同定とその効果的破綻予防、治療法の開発に関する多施設共同研究

平成16年度～18年度　総合研究報告書

主任研究者　山岸　正和

平成19（2007）年4月

別紙２

総合研究報告書目次

目　　次

厚生労働科学研究費補助金（循環器病等生活習慣病対策総合研究事業）

（総合）研究報告書

冠動脈不安定粥腫の同定とその効果的破綻予防、治療法の開発に関する多施設共同研究

（主任）研究者　山岸正和　　金沢大学大学院医学系研究科・循環器内科

研究要旨：不安定狭心症、心筋梗塞などの急性冠症候群の発症基盤となる粥腫を未然に診断可能となれば臨床的にも大変意義深い。本多施設共同研究では、各個研究と共に、各施設において血管内超音波法により観察され、所定の基準に合致する冠動脈局所を暫定的な不安定粥腫として 932 例（男 760 例、 女 172 例、平均年齢 67.2 才） の登録を完了し、“前向き” 追跡を行った。その結果、７８例に虚血性イベントの発生をみた。かかる部位では、イベント非発生部位に比し、動脈硬化粥腫容積が有意に大であるとの成績を得た。また、各個研究においては、診断精度の向上、治療効果の評価および非侵襲的診断法開発などにおいての所定の成果を得た。

水野杏一　　日本医科大学北総病院循環器科教授
椎名　毅　　筑波大学大システム情報工学科教授
細川　博昭　国立病院機構豊橋医療ｾﾝﾀｰ研究部長
山田　直明　国立循環器病センター放射線科医長
小宮山伸之　埼玉医科大学循環器内科教授
浦澤　一史　時計台記念病院心臓センター長
廣　　高史　山口大学医学部第二内科助手
高山　忠輝　日本大学医学部循環器内科助手
大塚頼隆　　国立循環器病センター内科医師
角辻　暁　　野崎徳州会病院心臓センター長

A. 研究目的

不安定狭心症、心筋梗塞などの急性冠症候群において、破綻する可能性の高い粥腫を未然に診断することは意義深い。血管内超音波法は、粥腫特性などが評価可能であることから、診断法として注目されて来た。本共同研究では一定の基準に基づいて診断された粥腫を“前向き”に経過観察することにより、粥腫不安定化の要因を探索し、予防、治療法の立案に寄与しようとするものである

B. 研究方法

各施設における診断的冠動脈造影、冠動脈形成術施行に際して、冠動脈硬化病変部位を血管内超音波法で観察し、表１の基準に合致する冠動脈局所を暫定的に登録した。

C. 研究成果

平成 18 年度は 932 例(女性 172 例、平均年齢 67.2 才)が各施設から登録された。登録病変の血管内超音波指標の平均値は、全血管面積 14.9±5.5 mm^2, 粥腫面積 9.1±3.7 mm^2 粥腫面積 63.2±11.2%, 病変長 7.2±3.1mm, 病変容積 55.5±33.2mm^3 平均粥腫面積 9.3±3.1mm 拡大リモデリング 27%, 偏心性病変 64%, 石灰化 41%であった。経過中 78 例で虚血性イベントの再発をみた。興味あることに、イベント再発部では粥腫容積が有意に大であるとの成績を得た。各個研究においては、診断精度の向上、治療効果の評価および非侵襲的診断法開発などにおいての所定の成果を得た。

表１

（１）血管造影法での狭窄率が５０％未満の病変。
（２）血管内超音波像の指標に加えて、形態的特徴として、既存の粥腫破綻、血栓の局在、石灰化の局在などを明記した。

（倫理面への配慮）

血管内超音波法による冠動脈評価は既に確立されたものである。本研究の遂行については、各施設での倫理委員会で審査された。

D. 結論

予後調査の結果、局所動脈硬化粥腫容積が大であるほど、経過中、虚血性イベントの再発し易いとの成績を得た。今後はかかる粥腫情報の非侵襲的診断への応用が期待されよう。

E. 研究発表

１． 学会発表

山岸正和他、第５４回日本心臓病学会学術集会シンポジウム２００６年９月、鹿児島

F. 知的所有権の取得状況

１． 特許取得

残留物回収装置（血管内ステント回収装置）特願 2004-259488

エフォリン及び/又はエフからなる炎症細胞の化学遊走調節剤及びその用途。特願 2006-92715

別紙４

研究成果の刊行に関する一覧表

書籍

著者氏名	論文タイトル名	書籍全体の編集者名	書　籍　名	出版社名	出版地	出版年	ページ
椎名毅	超音波	遠藤真広、西臺武弘	放射線物理学	オーム社	東京	2006	202頁
山岸正和	IVUS elastography	本江純子 斉藤　聡	IVUS マニュアル	中山書店	東京	2006	301
高山忠輝	IVUSによる冠動脈病変の安定と退縮について	本江純子 斎藤　穎	IVUS マニュアル	中山書店	東京	2006	244-249
寺島充康 山岸正和	IVUSによる不安定プラークの診断とその根拠	堀　正二	冠動脈疾患の New Concept	中山書店	東京	2006	65-71
野末　剛 川尻　剛照 井野　秀一 山岸　正和	冠動脈内エコーで何を評価できるか	小川　久雄	慢性冠動脈疾患の臨床	中山書店	東京	2006	134-143

雑誌

発表者氏名	論文タイトル名	発表誌名	巻号	ページ	出版年
Shina　T, Nitta N, Endo H, Yamagishi M	Assessment of　vulnerable coronary　plaque by intravascular　elasticity imaging	Proc. of IEEE International Ultrasonics, Ferroelectrics and Frequency　Control 50th Anniversary Joint Conference,		pp.364-367	2004年
Takano M, Inami S, Mizuno K.	Angioscopic follow-up study of coronary rupturedplaques in nonculprit lesions	J Am Coll Cardiolo	45	pp 652-658	2005年
Inami　S, Okamatsu K, Mizuno　K	Effect of statins on circulating oxidized low-density lipoprotein patients with hypercholesterolemia	Jpn Heart J	45	pp 969-975	2004年
Li Y, Honye J, Takayama T, Kanmatsuse K	Variability in quantitative measurement of the same segment with two different intravascular ultrasound systems: In vivo and in vitro studies	Catheterization and cardiovascular Interventions	62	175-180	2004年
Li Y, Honye J, Takayama T, Satoshi S	Intravascular ultrasound evaluation of ruptured plaque in the left main coronary artery misinterpreted as an aneurysm by angiography.	Catheterization and cardiovascular Interventions	63	314--316	2004年
高山忠輝	積極的脂質低下による冠動脈病変の安定化と退縮についての検討	日本循環器学会専門医誌	12巻 第2号	207－211	2004年

Murashige A, Hiro, T 他	Detection of Lipid-laden Atherosclerotic Plaque by Wavelet Analysis of Radio-frequency Intravascular Ultrasound Signals: In Vitro Validation and Preliminary In Vivo Application	Journal of the American College of Cardiology	Jun 21;45 (12)	pp1954-60	2005年
Kosuge M, Kimura K, Kojima S, Sakamoto T, Ishihara M, Asada Y, Tei C, Miyazaki S, Sonoda M, Tsuchihashi K, Yamagishi M, Ikeda Y, Shirai M, Hiraoka H, Inoue T, Saito F, Ogawa H;	On behalf of the Japanese Acute Coronary Syndrome Study (JACSS) Investigators.	Circ J	Oct;15 0(4)	pp.814-20	2005年
Maruo T, Nakatani S, Kanzaki H, Kakuchi H, Yamagishi M, Kitakaze M, Ohe T, Miyatake K.	Circadian variation of endothelial function in idiopathic dilated cardiomyopathy.	Am J Cardiol	Mar 1;97(5)	pp.699-702	2006年
Lazarevic AM, Nakatani S, Okita Y, Marinkovic J, Takeda Y, Hirooka K, Matsuo H, Kitamura S, Yamagishi M, Miyatake K.	Determinants of rapid progression of aortic root dilatation and complications in Marfan syndrome.	Int J Cardiol	Jan 13:106 (2)	pp.177-82	2006年
Higashikata T, Yamagishi M, Higashi T, Nagata I, Iihara K, Miyamoto S, Ishibashi-Ueda H, Nagaya N, Iwase T, Tomoike H, Sakamoto A.	Altered expression balance of matrix metalloproteinases and their inhibitors in human carotid plaque disruption: results of quantitative tissue analysis using real-time RT-PCR method	Atherosclerosis	Mar;18 5(1)	pp.165-72	2006年
Yamagishi M, Higashikata T, Ishibashi-Ueda H, Sasaki H, Ogino H, Iihara K, Miyamoto S, Nagaya N, Tomoike H, Sakamoto A.	Sustained upregulation of inflammatory chemokine and its receptor in aneurysmal and occlusive atherosclerotic disease: results form tissue analysis with cDNA macroarray and real-time reverse transcriptional polymerase chain reaction methods.	Circ J.	Dec;69 (12)	pp.1490-5	2005年
Ishihara M, Kojima S, Sakamoto T, Asada Y, Tei C, Kimura K, Miyazaki S, Sonoda M, Tsuchihashi K, Yamagishi M, Ikeda Y, Shirai M, Hiraoka H, Inoue T, Saito F, Ogawa H	Japanese Acute Coronary Syndrome Study Investigators. Acute hyperglycemia is associated with adverse outcome after acute myocardial infarction in the coronary intervention era.	Am Heart J	Oct;15 0(4)	pp.814-20	2005年
Saito S, Kobayashi J, Tagusari O, Bando K, Niwaya K, Nakajima H, Yamagishi M, Yagihara T, Kitamura S.	Successful excision of a cystic tumor of the atrioventricular nodal region	Circ J	Oct;69 (10)	pp.1293-4	2005年
Higo S, Uematsu M, Yamagishi M, Ishibashi-Ueda H, Awata M, Morozumi T, Ohara T, Nanto S, Nagata S.	Elevation of plasma matrix metalloproteinase-9 in the culprit coronary artery in patients with acute myocardial infarction: clinical evidence from distal protection.	Circ J	Oct;69 (10)	pp.1180-5	2005年

Nagaya N, Kangawa K, Itoh T, Iwase T, Murakami S, Miyahara Y, Fujii T, Uematsu M, Ohgushi H, Yamagishi M, Tokudome T, Mori H, Miyatake K, Kitamura S.	Transplantation of mesenchymal stem cells improves cardiac function in a Rat model of dilated cardiomyopathy.	Circulation	Aug 23 112(8)	pp.1128-35	2005年
Kojima S, Sakamoto T, Ishihara M, Kimura K, Miyazaki S, Yamagishi M, Tei C, Hiraoka H, Sonoda M, Tsuchihashi K, Shimoyama N, Honda T, Ogata Y, Matsui K, Ogawa H	Japanese Acute Coronary Syndrome Study (JACSS) Investigators. Prognostic usefulness of serum uric acid after acute myocardial infarction (the Japanese Acute Coronary Syndrome Study).	Am J Cardiol	Aug 15 96(4)	pp.489-95	2005年
Kosuge M, Kimura K, Kojima S, Sakamoto T, Ishihara M, Asada Y, Tei C, Miyazaki S, Sonoda M, Tsuchihashi K, Yamagishi M, Ikeda Y, Shirai M, Hiraoka H, Inoue T, Saito F, Ogawa H	Japanese Acute Coronary Syndrome Study (JACSS) Investigators. Beneficial effect of preinfarction angina on in-hospital outcome is preserved in elderly patients undergoing coronary intervention for anterior acute myocardial infarction.	Circ J	Jun;69(6)	pp.630-5	2005年
Kosuge M, Kimura K, Kojima S, Sakamoto T, Matsui K, Ishihara M, Asada Y, Tei C, Miyazaki S, Sonoda M, Tsuchihashi K, Yamagishi M, Ikeda Y, Shirai M, Hiraoka H, Inoue T, Saito F, Ogawa H;	Japanese Acute Coronary Syndrome Study (JACSS) Investigators. Effects of glucose abnormalities on in-hospital outcome after coronary intervention for acute myocardial infarction.	Circ J	Apr;69 (4)	pp.375-9	2005年
Ogata T, Yasaka M, Yamagishi M, Seguchi O, Nagatsuka K, Minematsu K	Atherosclerosis found on carotid ultrasonography is associated with atherosclerosis on coronary intravascular ultrasonography.	J Ultrasound Med	Apr;24 (4)	pp.469-74	2005年
Nitta N, Homma K, Shiina T	Intravascular Shear Stress Imaging Based on Ultrasonic Velocity Vector Measurement	Proc. of 2005 IEEE Ultrasonics Symposium		pp.520-523	2005年
Osaka T, Matsumura T, Mitake T, Nakatani T, Shiina T	Preliminary Results of Elasticity Imaging to Aortic Plaque	Proc. of the Fourth International Conference on the Ultrasonic Measurement and Imaging of Tissue Elasticity.	Vol.4	p.84	2005年
椎名　毅、山岸正和	血管内超音波エラストグラフィ	循環器科	Vol.57, No.5	pp.435-439	2005年
椎名　毅	最先端の超音波－ストレイン法でみる血管評価－	心エコー	Vol.6, No.10	pp.966-973	2005年
椎名　毅、新田尚隆、中谷敏、山岸正和	ストレインパワーイメージングによる冠動脈・大動脈プラーク性状の評価	第16回日本心血管画像動態学会抄録			2005年
椎名　毅、山岸正和	冠動脈イメージングの新技術：IVUS Elastography	Heart View	Vol.10, No.3		2006年

椎名　毅、新田尚隆、山岸正和	画像診断の進歩：血管超音波elastography	第14回コンピュータ外科学会講演論文集			2005年
Akihiro Murashige, Takafumi Hiro, Takashi Fujii et al.	Detection of Lipid-laden Atherosclerotic Plaque by Wavelet Analysis of Radio-frequency Intravascular Ultrasound Signals: In Vitro Validation and Preliminary In Vivo Application.	J Am Coll Cardiol	45	pp1954-60	2005年
Kouji Imoto, Takafumi Hiro, Takashi Fujii et al.	Longitudinal structural determinants of atherosclerotic plaque vulnerability: a computational analysis of stress distribution using vessel models and three-dimensional intravascular ultrasound imaging.	J Am Coll Cardiol	46	pp1507-15	2005年
Li Y, Honye J, Takayama T, Yokoyama S, Saito S.	A potential complication of directional coronary atherectomy for in-stent restenosis	Tex Heart Inst J	32(1).	pp108-109	2005年
Sato Y, Matsumoto N, Yoda S, Kunimoto S, Kasamaki Y, Takayama T, Furuhashi S, Takahashi M, Uchiyama T, Saito S	Whole-heart coronary magnetic resonance angiography in a patient with unstable angina.	Int J Cardiol	June		2005年
A. Itoh , E. Ueno, E. Tohno, H. Kamma , H.Takahashi , T. Shiina, M.Yamakawa, T. Matsumura	Breast Disease : Clinical Application of Ultrasound Elastography for Diagnosis	Radiology	Vol.231, No.2	pp.341-350	2006
N.Nitta, K.Homma, T.Shiina	Preasuure Gradient Estimation Based on Ultrasonic Blood Flow Measurement	Japanese Journal of Applied Physics	Vol.45, No.5B	pp.4740-4748	2006
Katsuda Y, Asano A, Murase Y, Chujo D, Yagi K, Kobayashi J, Mabuchi H, Yamagishi M	Association of Genetic Variation of the Adiponectin gene with Body Fat Distribution and Carotid Atherosclerosis in Japanese Obese Subjects	J Atheroscler Thromb	Vol.14 No.1	19-26	2007
Nohara A, Kawashiri MA, Claudel T, Mizuno M, Tsuchida M, Takata M, Katsuda S, Miwa K, Inazu A, Kuipers F, Kobayashi J, Koizumi J, Yamagishi M, Mabuchi H	High Frequency of a Retinoid X Receptor {gamma} Gene Variant in Familial Combined Hyperlipidemia That Associates With Atherogenic Dyslipidemia	Arterioscler Thromb Vasc Biol	Vol.27	923-928	2007
Takata M, Inazu A, Katsuda S, Miwa K, Kawashiri MA, Nohara A, Higashikata T, Kobayashi J, Mabuchi H, Yamagishi M	CETP (cholesteryl ester transfer protein) promoter -1337 C>T polymorphism protects against coronary atherosclerosis in Japanese patients with heterozygous familial hypercholesterolaemia	Clin Sci (Lond)	Vol.111 No.5	325-31	2006
Gojo S, Kyo S, Nishimura S, Komiyama N, Kawai N, Bessho M, Sato H, Asakura T, Nishimura M, Ikebuchi K	Cardiac resurrection after bone-marrow-derived mononuclear cell transplantation during left ventricular assist device support	Ann Thorac Surg	Vol.83 No.2	661-2	2007

Yoshida T, Kobayashi Y, Nakayama T, Kuroda N, Komiyama N, Komuro I	Stent deformity caused by coronary artery spasm	Circ J	Vol.70 No.6	800-1	2006
Funabashi N, Komiyama N, Asano M, Komuro I	Endocardial fibrosis in subacute non-Q wave myocardial infarction demonstrated by multislice computed tomography	Int J Cardiol	Vol.109 No.3	430-1	2006
Koizumi T, Yokoyama M, Namikawa S, Kuriyama N, Nameki M, Nakayama T, Kaneda H, Sudhir K, Yock PG, Komiyama N, Fitzgerald PJ	Location of focal vasospasm provoked by ergonovine maleate within coronary arteries in patients with vasospastic angina pectoris	Am J Cardiol	Vol.97 No.9	1322-5	2006
Ishibashi F, Yokoyama S, Miyahara K, Dabreo A, Weiss ER, Iafrati M, Takano M, Okamatsu K, Mizuno K, Waxman S	Quantitative colorimetry of atherosclerotic plaque using the L*a*b* color space during angioscopy for the detection of lipid cores underneath thin fibrous caps	Int J Cardiovasc Imaging			2007
Takano M, Ohba T, Inami S, Seimiya K, Sakai S, Mizuno K	Angioscopic differences in neointimal coverage and in persistence of thrombus between sirolimus-eluting stents and bare metal stents after a 6-month implantation	Eur Heart J	Vol.27 No.18	2189-95	2006
Seimiya K, Inami S, Takano M, Ohba T, Sakai S, Takano T, Mizuno K	Significance of plaque disruption sites in acute coronary syndrome	J Nippon Med Sch	Vol.73 No.3	141-8	2006
Li Y, Fukuda N, Kunimoto S, Yokoyama S, Hagikura K, Kawano T, Takayama T, Honye J, Kobayashi N, Mugishima H, Saito S, Serie K	Stent-based delivery of antisense oligodeoxynucleotides targeted to the PDGF A-chain decreases in-stent restenosis of the coronary artery	J Cardiovasc Pharmacol	Vol.48 No.4	184-90	2006
Li Y, Honye J, Takayama T, Saito S	Generalized spasm of the right coronary artery after successful stent implantation provoked by intracoronary administration of ergonovine	Int J Cardiol			2006
Sato Y, Ichikawa M, Nakanishi K, Matsumoto N, Yoda S, Kasamaki Y, Takayama T, Koyama Y, Inoue F, Takahashi M, Uchiyama T, Saito S	Multidetector computed tomography of a saphenous vein graft aneurysm	Heart Vessels	Vol.21 No.2	135-6	2006
Sato Y, Inoue F, Kunimasa T, Matsumoto N, Yoda S, Tani S, Takayama T, Uchiyama T, Tanaka H, Furuhashi S, Takahashi M, Koyama Y, Saito S	Diagnosis of anomalous origin of the right coronary artery using multislice computed tomography: evaluation of possible causes of myocardial ischemia	Heart Vessels	Vol.20 No.6	298-300	2005

Takayama T, Hiro T, Yamagishi M, Daida H, Saito S, Yamaguchi T, Matsuzaki M	Rationale and design for a study using intravascular ultrasound to evaluate effects of rosuvastatin on coronary artery atheroma in Japanese subjects: COSMOS study (Coronary Atherosclerosis Study Measuring Effects of Rosuvastatin Using Intravascular Ultrasound in Japanese Subjects).	Circulation journal	Vol.71 No.2	271-275	2007
Hata M, Sezai A, Niino T, Yoda M, Wakui S, Chiku M, Takayama T, Honye J, Saitoh S, Minami K	What is the optimal management for preventing saphenous vein graft diseases?: early results of intravascular angioscopic assessment.	Circulation journal	Vol.71 No.2	286-287	2007
Tanaka M, Goto Y, Suzuki S, Morii I, Otsuka Y, Miyazaki S, Nonogi H	Postinfarction cardiac rupture despite immediate reperfusion therapy in a patient with severe aortic valve stenosis	Heart Vessels	Vol.21 No.1	59-62	2006
Yamada N, Higashi M, Otsubo R, Sakuma T, Oyama N, Tanaka R, Iihara K, Naritomi H, Minematsu K, Naito H	Association between signal hyperintensity on T1-weighted MR imaging of carotid plaques and ipsilateral ischemic events	AJNR Am J Neuroradiol	Vol.28 No.2	287-92	2007
Sakai H, Oyama N, Kishimoto N, Takahashi M, Urasawa K, Tsutsui H	Revascularization of Malignant Coronary Instent Restenosis Resulting From Takayasu's Arteritis Using Sirolimus-Eluting Stents	Int Heart J	Vol.47 No.5	795-801	2006

Assessment of Vulnerable Coronary Plaque by Intravascular Elasticity Imaging

Tsuyoshi Shiina[1], Naotaka Nitta[2], Hiroyuki Endo[1] and Masakazu Yamagishi[3]

[1] Graduate school of Systems and Information Engineering, University of Tsukuba, Tsukuba 305-8573, Japan
[2]Institute for Human Science and Biomedical Engineering, National Institute of Advanced Industrial Science and Technology, Tsukuba 305-8564, Japan
[3] National Cardiovascular Center, Osaka, Japan

Abstract — Plaque rupture is regarded as one of main causes of acute coronary syndromes. To prevent plaque rupture and guide a pharmacological treatment, it is important to image the weak (fragile) part of atheroscleotic plaque. Our preliminary experiments revealed the feasibility of stain image using IVUS to discriminate between different types of plaque. In this paper, for the purpose of obtaining more fine and stable assessments of vulnerable plaque under interventional conditions, we propose a strain power image as an index of tissue deformability by analyzing the time-varying strain profiles obtained from the IVUS data. We also conducted *in vivo* test with a new acquisition device that allows us to capture a large scale of RF data. And its results demonstrated that the strain power imaging has the potential to evaluate the vulnerability of plaques

I. Introduction

Assessment of vulnerable coronary plaque is an essential procedure for prevention of the acute ischemic syndromes due to plaque rupture. In order to assess any risk factors of plaque rupture such as the lipid rich plaque and the vulnerability of fibrous cap, the intravascular elasticity imaging by intravascular ultrasound (IVUS) is an useful technique different from the conventional IVUS echograms because the plaque compositions such as lipid, fibrosis and calcification can be viscerally assessed by the difference of tissue stiffness[1]. We also previously reported the usefulness of intravascular elasticity (strain) imaging based on our method which had a high ability to precisely detect strain over a large dynamic range from RF data acquired during interventional procedures [2].

However, the spatial resolution and accuracy of the intravascular strain imaging became blurred when catheter rotation induced by heart beat was severe. Then, for the purpose of obtaining more fine and accurate assessments of any plaques under interventional conditions, we newly propose the strain power imaging by analyzing the time-varying strain profiles. For each point or region of interest (ROI) on the instantaneous strain images obtained between consecutive pairs of echograms, strain profiles as a function of time are obtained by two-dimensionally tracking the ROI. Next, the strain power around heart beat frequency is calculated from the power spectrum of the strain profiles over a single cardiac cycle. The usefulness of the method was evaluated by using large amount of echogram frame data acquired during interventional procedure. In this paper, a concept of strain power imaging is proposed and some results using RF data acquired during interventional procedure are presented.

II. Principle of Strain Power Imaging

Plaque rapture is related to a fragility of the thin fibrous cap over lipid core. These fragile parts of vulnerable plaque are expected to be more deformable under variation of blood pressure and imaged as high strain area. In order to detect vulnerable location by evaluating the deformability of plague, we propose strain power image by IVUS.

Since the change of artery diameter due to blood pressure induces local deformation (strain) of the arterial wall inside, which corresponds to elasticity, strain should discriminate the plaque type. However, the strain magnitude at any ROI periodically changes according to time-varying blood pressure due to heart beat and the instantaneous strain image represents different pattern at each phase of cardiac cycle. Therefore, the anatomically-correct region of plaque cannot be identified because of time-varying strain

0-7803-8412-1/04/$20.00 (c)2004 IEEE.

2004 IEEE International Ultrasonics, Ferroelectrics, and Frequency Control Joint 50th Anniversary Conference

distribution. Therefore, time-invariant intravascular strain imaging independently of heart beat is required for accurate identification of plaque expansion.

On the other hand, the spatial resolution and the accuracy of intravascular strain imaging also become blurred if the undesired catheter and artery rotations induced by heart beat is severe during interventional operation. Therefore, these rotations must be compensated laterally in measuring the radial displacement for accurate radial strain estimate.

In order to overcome the above two restriction, that is, the time-varying strain profile and the catheter and artery rotations, we propose a concept of the strain power imaging based on two-dimensional (2-D) search of any ROI in this study. This concept is briefly explained below.

We previously proposed a technique for estimating strain distribution, which is referred to as the combined autocorrelation method (CAM) [3]. CAM consists of two-step estimation, that is, coarse and fine estimation using the outputs of a quadrature detector between consecutive pairs of echograms. Consequently, CAM has a potential for rapid and accurate estimate radial strain over a wide dynamic range. For compensating the rotations, CAM was modified for coping with catheter and artery rotations, that is, the discrepancy of compared two scan lines is compensated by the 2-D correlation search in the radial and lateral directions. As a result, accurate radial displacement distribution $v_r(r,\theta,t)$ at time t can be measured, and instantaneous strain distribution $\varepsilon_r(r,\theta,t)$ between adjacent two frames can be also estimated without influence of catheter and artery rotations as follows:

$$\varepsilon_r(r,\theta,t)=\frac{\partial v_r(r,\theta,t)}{\partial r} \qquad (1)$$

As mentioned above, this strain profile $\varepsilon_r(r,\theta,t)$ is time-varying according to heart beat, and the strain mapping also changes periodically in same dynamic range. For identifying the expansion of plaque independently of periodic change of strain, power spectrogram of the traced instantaneous strain profile at any ROI is introduced. Strain profile at any ROI mainly includes heart beat frequency component (about 1 Hz). Therefore, at any time, the magnitude of power spectrum around heart beat frequency should be time-invariant. Note that the strain profile at any ROI should be traced by using the 2-D search because the ROI moves to different position from the initial one according to heart beat. For the traced strain profile $\hat{\varepsilon}_r(r,\theta,t)$, power spectrogram $p(r,\theta,t;2\pi f)$ can be obtained as follows:

$$p(r,\theta,t;2\pi f)=\left|\int_{-t_0/2}^{t_0/2}\hat{\varepsilon}_r(r,\theta,t+t')e^{-j2\pi ft'}dt'\right|^2 \qquad (2)$$

where t_0 is the time duration of Fourier transform and should be determined by referring a single cardiac cycle time period (about 1 sec). Since this power spectrogram has a time-invariant main peak around heart beat frequency as mentioned above, we can obtain the time-invariant strain power image by mapping the power around heart beat frequency f_0 at any ROI as follows:

$$P(r,\theta,t)=\int_{f_c-\Delta f}^{f_c+\Delta f}p(r,\theta,t;2\pi f)df \qquad (3)$$

where Δf is the duration frequency for strain power imaging. Consequently, we can obtain high-resolution and stable strain images at low fluctuation of strain pattern independently of cardiac cycle and identify the expansion of plaque accurately and precisely.

III. In Vivo Examination of Coronary Arteries

For evaluating the feasibility of the proposed strain power imaging, a prototype of the imaging system was developed for in vivo IVUS examination of coronary arteries. The system consists of a IVUS catheter with a center frequency of 40 MHz (Terumo Co. Ltd, Japan) and the custom-made A/D converter with huge deep memory (1.6GB) as shown in Fig.1. The successive frame data, which consists of 1024 RF scan lines, were acquired by this A/D converter at a frame rate of 30 Hz and a sampling rate of 240 MHz and 12 bits. The

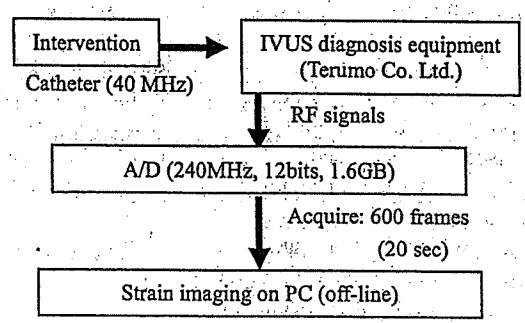

Fig.1: Elasticity imaging system with IVUS for clinical examination.

memory of 1.6 GB allows the capture of 600 frames, which corresponds to the duration of 20 second, for an investigation depth of 5 mm. Such deep memory is required for the movie display of multiple strain power images because one strain power images is constructed by at least 1 second duration as mentioned above with respect to eq.(2). The movie display can reveal the validness of time-invariant strain power imaging independently of heart beat.

In vivo tests during interventional procedure were conducted for several patients suffering from the coronary plaques. After acquiring RF data from the IVUS catheter using the custom-made A/D converter during interventional procedures, many frames of instantaneous strain image were calculated by applying the modified CAM for consecutive pairs of echograms. Based on all instantaneous strain images, strain profile during a cardiac cycle at each ROI was obtained by tracing the ROI throughout consecutive instantaneous strain images during a cardiac cycle using 2-D displacement vector calculated by the 2-D correlation search. Strain profiles were Fourier transformed by eq.(2), and the strain powers at all ROI calculated by eq.(3) were mapped as strain power image. By repeating the above processing at every key frame of instantaneous strain image, multiple strain power images can be obtained.

Figure 2 shows the B-mode image of the complex plaque type of the left coronary artery with fibro-cellular plaque and calcification. The area of fibro-cellular plaque is laid from 12 to 4 o'clock and the calcification can be seen as the high-intensity area with a shadow at 6 o'clock. Figure 3(a) and (b) show the instantaneous radial strain images obtained at the transition phase from diastole to systole and at the diastolic phase. These images were displayed by color-coding of the absolute value of strain between 0 and 1.5 %, which correspond to blue (hard) and red (soft), respectively, and superimposed on the B-mode image. The above strain threshold eliminated some artifact due myocardium and areas of blood. Consequently, the boundary between lumen and arterial wall appears more clearly than B-mode image. And the calcification in these images can be observed as the lower strain area than the fibro-cellular area. However, the strain distribution at the transition phase shown in Fig.3(a) is different from that at the diastolic phase shown in Fig.3(b) because strain distribution varies according to cardiac motion. Even if the optimum dynamic range for individual each strain image is selected, the same patterns cannot be always displayed because the vessel wall generally exhibits nonlinear elasticity.

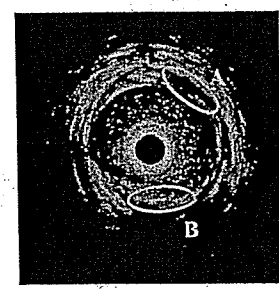

Fig.2: B-mode image of the left coronary artery with the complex type plaques of fibro-cellular plaque and calcification.

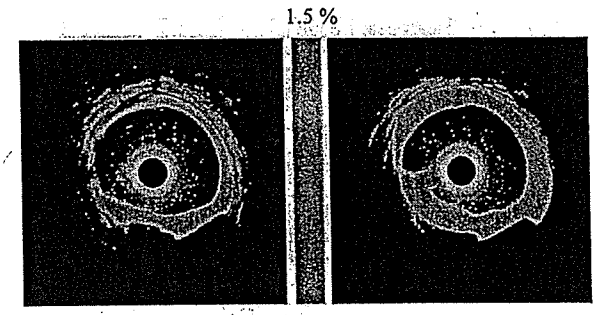

Fig.3: Instantaneous strain images during a cardiac cycle. (a) is obtained at the transition phase from diastole to systole and (b) is obtained at the diastolic phase.

In order to obtain the strain profiles of ROIs marked as A (fibro-cellular plaque) and B (calcification) in Fig.2 respectively, each ROI was traced by using the measured 2-D displacement vectors in estimating strain distribution. The obtained strain profiles, which is the averaged strain within each ROI, were plotted as a function of time, as shown in Fig.4(a). Although the amplitude of strain profile of the fibro-cellular plaque is entirely larger than that of the calcification, the same level of both profiles can be locally observed. Figure 3(a) and (b) were obtained at the phases indicated as "Fig.3(a)" and "Fig.3(b)" in Fig.4(a), respectively. Figure 4(b) indicates the power spectrum of strain profile shown in Fig.4(a). The fibro-cellular plaque can be clearly separated from the calcification as the difference of strain power around heart beat rate of 1Hz. Figure 5 shows the strain power image, which locally maps the strain power around heart beat rate of 1 Hz shown in Fig.4(b). We can evaluate the deformability of the soft fibro-cellular plaque and the hard calcification, and clearly identify the expansion area of calcification independently of heart beat in strain power imaging.

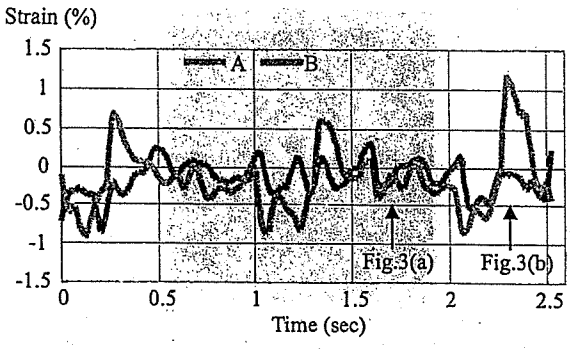

(a)

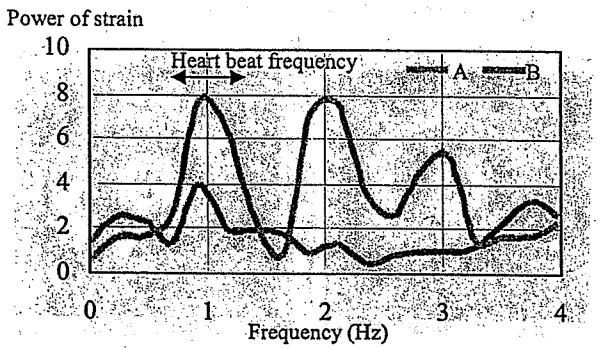

(b)

Fig.4: (a)Strain profile and (b)its power spectrum at ROI A and B marked in Fig.2.

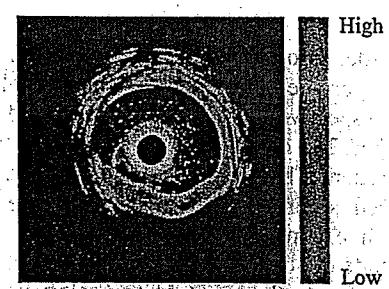

Fig.5: Strain power image of the left coronary artery with the complex type plaques.

Finally, Fig.6 shows the example of in vivo test for vulnerable coronary plaque. From the B-mode image shown in Fig.6(a), the existence of vulnerable plaque was predicted from 10 to 3 o'clock. Fig.6(b) indicates the strain power image. As predicted in B-mode image, strain power imaging is almost time-invariant and the vulnerable plaque can be observed as the soft area

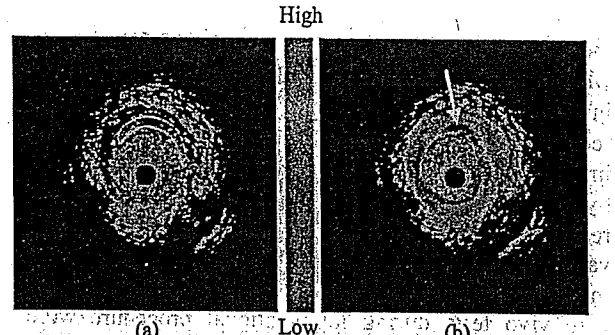

Fig.6: Strain power image for vulnerable coronary plaque. (a) indicates the B-mode and (b) shows the strain power image.

independently of heart beat motion. These results revealed that the strain power imaging is useful for stably discriminating different types of plaque without the influence of cardiac motion during intervention.

IV. Conclusions

In this paper, a strain power imaging based on the elasticity imaging using IVUS was proposed for diagnosing the plaque types of coronary arteries. A measurement system for clinical examination was developed and in vivo tests during interventional procedure were conducted for several patients. Results demonstrate that different types of plaque can be discriminated without the influence of cardiac motion by strain power imaging.

In future work, we must acquire more clinical data and investigate the statistical classification of plaques by strain power imaging. Moreover, strain power image must be compared with its histology for validating the usefulness of the proposed method.

Acknowledgement : This research is partly supported by grants of National Cardiovascular Center, Japan.

References

[1] J. A. Shaar, C. L. de Korte *et al.*, "Characterizing Vulnerable Plaque Features with Intravascular Elastography" Circulation 108 2636-2641 2003

[2] T Shiina N Nitta M Yamagishi "Coronary Arteries Characterization Based on Tissue

Autocorrelation Processing." Proc.of 1996 IEEE Ultrasonics Symp. 1331-1336. 1996.

Journal of the American College of Cardiology
© 2005 by the American College of Cardiology Foundation
Published by Elsevier Inc.

Vol. 45, No. 5, 2005
ISSN 0735-1097/05/$30.00
doi:10.1016/j.jacc.2004.09.077

CLINICAL RESEARCH **Coronary Artery Disease**

Angioscopic Follow-Up Study of Coronary Ruptured Plaques in Nonculprit Lesions

Masamichi Takano, MD, Shigenobu Inami, MD, Fumiyuki Ishibashi, MD, Kentaro Okamatsu, MD, Koji Seimiya, MD, Takayoshi Ohba, MD, Shunta Sakai, MD, Kyoichi Mizuno, MD, PHD, FACC
Chiba, Japan

OBJECTIVES Changes of ruptured plaques in nonculprit lesions were evaluated using coronary angioscopy.

BACKGROUND The concept of multiple coronary plaque ruptures has been established. However, no detailed follow-up studies of ruptured plaques in nonculprit lesions have yet been reported.

METHODS Forty-eight thrombi in 50 ruptured coronary plaques in nonculprit lesions in 30 patients were identified by angioscopy. The percent diameter stenosis (%DS) at the target plaques on quantitative coronary angiographic analysis and the serum C-reactive protein (CRP) level were measured.

RESULTS The mean angioscopic follow-up period was 13 ± 9 months. Thirty-five superimposed thrombi still remained at follow-up, and the predominant thrombus color changed from red (56%) at baseline to pinkish-white (83%) at follow-up. The healing rate increased according to the angioscopic follow-up period (23% at ≤12 months vs. 55% at >12 months, $p = 0.044$). The %DS at the healed plaque increased from baseline to follow-up (12.3 ± 5.8% vs. 22.7 ± 11.6%, respectively; $p = 0.0004$). The serum CRP level in patients with healed plaques ($n = 10$) was lower than that in those without healed plaques ($n = 19$; 0.07 ± 0.03 mg/dl vs. 0.15 ± 0.11 mg/dl, respectively; $p = 0.007$).

CONCLUSIONS The present study demonstrated that: 1) ruptured plaques in nonculprit lesions tend to heal slowly with a progression of angiographic stenosis; and 2) the serum CRP level might reflect the disease activity of the plaque ruptures. (J Am Coll Cardiol 2005;45:652–8) © 2005 by the American College of Cardiology Foundation

Atherosclerotic coronary plaque rupture (or erosion) and subsequent thrombus formation in the culprit lesion are recognized to be the major motivating factors in acute coronary syndrome (ACS) (1–5). Intravascular ultrasound (IVUS) studies recently reported that a plaque rupture occurs not only in culprit lesions but also in other atherosclerotic plaques in patients with ACS, stable angina pectoris (SAP), and silent myocardial ischemia (6–9). The concept of "pancoronaritis" or "multifocal plaque rupture" has been established. In the clinical setting, ruptured plaque in the culprit lesion is usually treated with percutaneous coronary intervention (PCI), and the natural course of ruptured plaque without PCI has not yet been reported. Previous pathologic studies have shown that healed plaques after a subclinical rupture tend to result in increased narrowing of the coronary lumen (10,11). Nevertheless, ruptured plaques in nonculprit lesions have not been well described as to whether they heal uneventfully with (or without) luminal narrowing or lead to an occurrence of acute coronary events in living patients.

See page 659

Serum C-reactive protein (CRP), a predictor of acute myocardial infarction (MI), is expressed in human atherosclerotic lesions, and most CRPs show an increased expression at sites of plaque rupture (12–14). The serial changes in the serum CRP level in patients with multiple plaque ruptures have also not yet been elucidated.

Coronary angioscopy can provide direct images of the endoluminal surface and detailed information on plaque rupture (or healing), as well as on the existence and age of a thrombus. The purpose of this study was to investigate the natural course of ruptured plaques in nonculprit lesions in living patients.

METHODS

Patient population. Between September 1998 and December 2003, 327 patients were analyzed by coronary angioscopy. Thirty consecutive patients in whom two or three de novo native coronary arteries were evaluated by repeat angioscopic procedures and who had ruptured plaque(s) at nonculprit lesions were enrolled in this study. Written, informed consent approved by our institutional review boards was obtained from all study patients before catheterization.

Clinical demographics. The patient demographics were obtained by a hospital chart review. Stable angina pectoris was defined as a positive stress test and no change in the frequency, duration, or intensity of symptoms lasting <4 weeks. Unstable angina pectoris (UAP) was new-onset

From the Department of Internal Medicine, Chiba-Hokusoh Hospital, Nippon Medical School, Chiba, Japan.

Manuscript received June 3, 2004; revised manuscript received September 8, 2004, accepted September 13, 2004.

Abbreviations and Acronyms

ACS = acute coronary syndrome
CRP = C-reactive protein
%DS = percent diameter stenosis
IVUS = intravascular ultrasound
LAD = left anterior descending coronary artery
LCx = left circumflex artery
MI = myocardial infarction
PCI = percutaneous coronary intervention
QCA = quantitative coronary angiogram
RCA = right coronary artery
SAP = stable angina pectoris
UAP = unstable angina pectoris

severe angina, accelerated angina, or rest angina. Acute or recent MI occurred within ≤6 weeks, and a previous MI >6 weeks. Patients with UAP, acute MI, and recent MI were categorized as ACS. Blood sampling was collected in the fasting state, immediately before each angioscopic procedure, except for CRP in patients with ACS. In ACS, the serum CRP level four weeks after onset was selected as the baseline level because of exclusion of the effects of myocardial necrosis.

A culprit lesion was identified by the combination of the electrocardiographic findings, left ventricle wall motion abnormalities (left ventriculography or echocardiography), scintigraphic defects, and angiographic lesion morphology.

Angiographic analysis. All angiograms were analyzed with a computer-assisted, automated edge-detection algorithm (CMS, MEDIS, Nuenen, The Netherlands) by an angiographer blinded to the clinical and angioscopic findings, using a standard qualitative definition and quantitative coronary angiographic (QCA) measurements. The variability of the QCA measurements was analyzed repeat measurements of the target plaques. The variation in minimal lumen diameter was 0.09 ± 0.09 mm and that in %DS was 2.8 ± 2.1%. A follow-up angiogram was obtained at the same angle as that in the baseline study.

Angioscopic imaging. The coronary angioscopic procedure has been previously reported (15). The proximal segments to the culprit lesion were observed by angioscopy before PCI for avoidance of mechanical damage due to the PCI procedure. The distal segments to the culprit lesion and the other coronary arteries were examined after PCI. The angioscopic and fluoroscopic images during the angioscopic observations were recorded on digital videotape for later analysis. The exact position of the angioscopic catheter at the site of the target plaque was recorded on an angiogram to ensure a reliable comparison.

Definition and analysis of angioscopic findings. A ruptured plaque was defined as a complex plaque and/or a superimposed thrombus. A complex plaque was considered to be present when the surface of the lesion had an irregular appearance, including a fissure, flap, and ulceration. Based on the surface color, the plaque was classified as either yellow or white. A fissure was defined as a torn intima without floating into the lumen; a flap was a disrupted fragment floating into the lumen; and ulceration was a crater-like lesion suggesting a gap in the vessel wall (Fig. 1). A thrombus was defined as a coalescent red or pinkish-white, superficial, or protruding mass adhering to the vessel surface, but clearly a separate structure that remained despite being flushed with saline solution. Complete plaque healing was defined as a covering by the neointima and the disappearance of thrombus and complex plaque.

The intra-observer agreement on angioscopic images was measured by having an observer repeat assessment of 20 images (presented in random order) after one week. The inter-observer agreement was measured by comparing the assessment of 100 images by the two observers blinded to the clinical background. The intra-observer agreements for the evaluated angioscopic items (complex plaque, yellow plaque, and thrombus) were 95%, 95%, and 100%, respectively. The inter-observer agreements of those items were 93%, 98%, and 97%, respectively. The kappa values for intra-observer agreement of them were 0.94, 0.99, and 0.95, respectively. The kappa values for inter-observer agreement of them were 0.95, 0.96, and 0.94, respectively. When there was any discordance between the two observers, a third investigator read the images, and a consensus was obtained.

Percutaneous coronary intervention and clinical follow-up. The PCI was performed for only the culprit lesions using a stent. Two kinds of antiplatelet agents—ticlopidine (200 mg/day) or cilostazole (200 mg/day), added to aspirin (81 to 200 mg/day)—were administered for at least six months. Glycoprotein IIb/IIIa inhibitors have not been approved for clinical use in Japan. Repeat PCI, bypass surgery, ACS, and death were all considered to be major outcome events.

Statistical analysis. Statistical analysis was performed with StatView 5.0 (SAS Institute, Cary, North Carolina). Categorical variables are presented as frequencies and compared

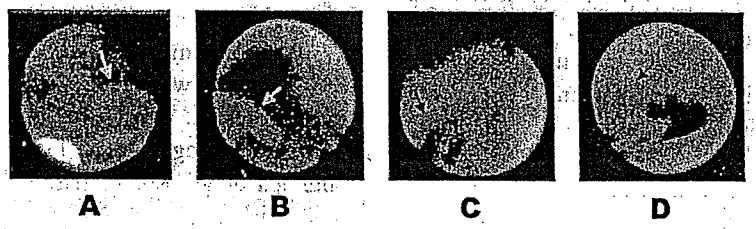

Figure 1. Angioscopic images of nonculprit ruptured plaques. (A) Yellow plaque with a fissure (arrow) and red thrombus. (B) Yellow plaque with a flap (arrow). (C) Yellow plaque with an ulceration (arrow) and red thrombus. (D) Yellow plaque with a pinkish-white thrombus (arrow).

JACC Vol. 45, No. 5, 2005
March 1, 2005:652–8

Table 1. Patient Characteristics at Baseline (n = 30)

Age (yrs)	59.3 ± 9.1
Gender, male	25 (83%)
Risk factors for atherosclerosis	
Diabetes mellitus	8 (27%)
Hypertension	17 (57%)
Hyperlipidemia	27 (90%)
Cigarette smoking	22 (73%)
Obesity	11 (37%)
Family history	6 (20%)
Diagnosis for ischemic heart disease	
Acute coronary syndrome	17 (57%)
Previous myocardial infarction	10 (33%)
Stable angina pectoris	3 (10%)
Location of PCI vessel	
Right coronary artery	10 (33%)
Left descending artery	12 (40%)
Left circumflex artery	8 (27%)
Number of diseased vessel(s)	
1	14 (47%)
2	15 (50%)
3	1 (3%)
Serum LDL-C level (mg/dl)	151 ± 31
Serum CRP level (mg/dl)	0.22 ± 0.22
Number of ruptured plaques in nonculprit lesions	
1	19 (63%)
2	4 (13%)
3	5 (17%)
4	2 (7%)

Data are presented as the mean value ± SD or number (%) of patients.
CRP = C-reactive protein; LDL-C = low-density lipoprotein cholesterol; PCI = percutaneous coronary intervention.

by the Fisher exact test. Continuous quantitative data are presented as the mean value ± SD. Continuous data were compared by the unpaired Student *t* test between the different categories and by the paired Student *t* test between the baseline and follow-up. Univariate logistic regression analysis was tested to determine clinical predictors for the healing of nonculprit ruptured plaques. Variables that achieved a significance of levels in a univariate logistic regression analysis were then selected for testing in a multivariate logistic regression analysis. A p value of <0.05 was considered to be statistically significant.

RESULTS

Clinical characteristics at baseline. The clinical characteristics of 30 patients at baseline are summarized in Table 1. Coronary angioscopy was performed in 73 arteries (2.4 arteries/patient): 25 right coronary arteries (RCA), 26 left anterior descending coronary arteries (LAD), and 22 left circumflex arteries (LCx).

Lesion characteristics at baseline. A total of 50 ruptured plaques were found in 36 arteries (19 in RCA, 8 in LAD, 9 in LCx). The lesion characteristics of the ruptured plaques are summarized in Table 2. The number of ruptured plaques in nonculprit lesions ranged from one to four per patient (1.67/patient) and 0.68/artery. The %DS of ruptured plaques was 16.3 ± 9.7%. Twenty-five (50%) of 50 plaques were recognized as complex lesions on the angiograms.

Table 2. Lesion Characteristics at Baseline

Ruptured Plaques in Nonculprit Lesions	n = 50
Distribution of ruptured plaques	
Right coronary artery	27 (54%)
Left anterior descending artery	13 (26%)
Left circumflex artery	10 (20%)
Angiographic measurements	
Reference diameter (mm)	3.07 ± 0.58
Minimal lumen diameter (mm)	2.63 ± 0.58
Percent diameter stenosis	16.3 ± 9.7
Angiographic morphology	
Wall irregularity	11 (22%)
Haziness or filling defect	12 (24%)
Ulceration	2 (4%)
No complexity	25 (50%)
Angioscopic findings	
Thrombus	48 (96%)
Red	28 (56%)
Pinkish-white	20 (40%)
Plaque	
Yellow plaque	46 (92%)
Fissure	22 (44%)
Flap	9 (18%)
Ulceration	6 (12%)

Data are presented as the mean value ± SD or number (%) of lesions.

Forty-eight ruptured plaques (96%) were accompanied by superimposed thrombi, and 56% were red thrombi. No superimposed thrombi could be detected in each plaque with a fissure and flap. There were 13 plaques in which the underlying ruptures were not visualized due to the superimposed thrombi. Forty-six ruptured plaques (92%) were diagnosed to be yellow plaques.

Table 3. Lesion Characteristics at Follow-Up

	Healed Plaques (n = 15)	Nonhealed Plaques (n = 35)
Distribution of ruptured plaques		
Right coronary artery	8 (53%)	19 (54%)
Left anterior descending artery	6 (40%)	7 (20%)
Left circumflex artery	1 (7%)	9 (26%)
Angiographic measurements		
Reference diameter (mm)	3.05 ± 0.45	3.07 ± 0.64
Minimal lumen diameter (mm)	2.53 ± 0.59	2.62 ± 0.63
Percent diameter stenosis	22.7 ± 11.6	19.1 ± 12.0
Angiographic morphology		
Wall irregularity	2 (13%)	9 (26%)
Haziness or filling defect	1 (7%)	8 (23%)
Ulceration	1 (7%)	1 (3%)
No complexity	11 (73%)	17 (51%)
Angioscopic findings		
Thrombus	0	35 (100%)
Red	—	6 (17%)
Pinkish-white	—	29 (%)
Plaque		
Yellow plaque	7 (47%)	34 (97%)
Fissure	0	16 (46%)
Flap	0	4 (11%)
Ulceration	0	2 (6%)

Data are presented as the number (%) of lesions or mean value ± SD.

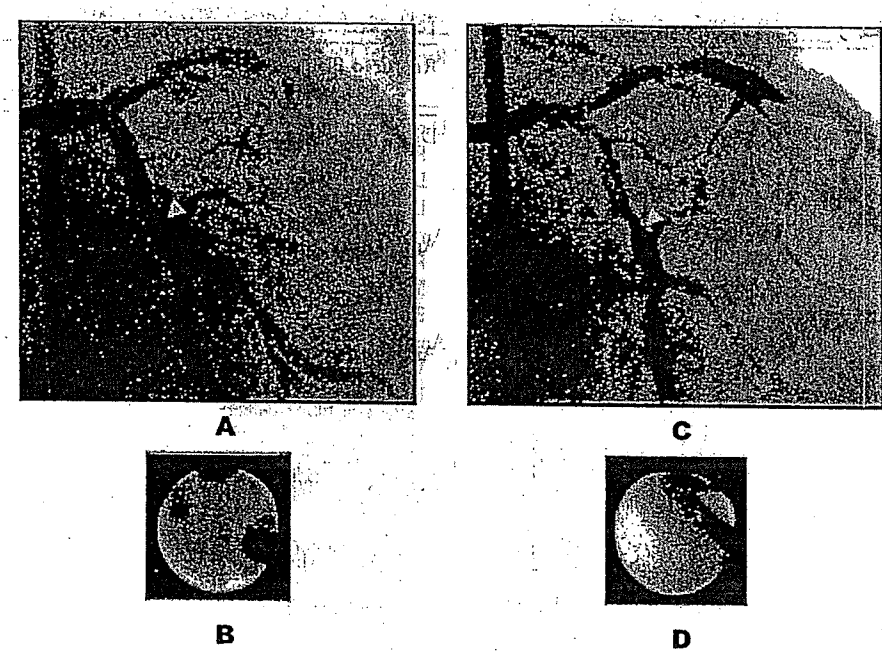

Figure 2. Healing of nonculprit plaque in acute coronary syndrome (ACS). (A) Coronary angiogram of the left circumflex artery (LCx) in a patient with ACS. (B) A pinkish-white thrombus on the yellow plaque was observed in the mid-portion of the LCx at baseline (white arrowhead in A). (C) A 12-month follow-up coronary angiogram in the same patient. (D) The thrombus disappeared and a smooth white intima was found (white arrowhead in C). In the quantitative coronary angiogram measurements, %DS at the angioscopic image site (white arrowhead in A and C) increased from 34.5% at baseline to 43.1% at follow-up.

Lesion characteristics at follow-up. Follow-up angioscopy was performed 13 ± 9 months after the baseline studies to document the changes in the nonculprit ruptured plaques that had been previously identified. At follow-up, 35 thrombi still remained on the same plaques at baseline (Table 3). The frequency of red thrombi decreased to 17%, and pinkish-white thrombi became predominant. Fifteen ruptured plaques in 11 patients healed completely (Fig. 2), and the overall healing rate of the plaque was 30%. The frequency of yellow plaques in the healed plaques was 47%. The healing rate of the plaque increased according to the follow-up period (23% [9 of 39] at ≤12 months vs. 55% [6 of 11] at >12 months, p = 0.044) (Fig. 3).

On QCA analysis, the %DS of the healed plaques at follow-up was greater than that at baseline (22.7 ± 11.6% vs. 12.3 ± 5.8%; p = 0.0004), whereas that of nonhealed plaque was not significantly different between that at follow-up and baseline (19.1 ± 12.0% vs. 18.0 ± 10.6%; p = 0.6).

Clinical characteristics at follow-up. In 29 patients, all plaques in the same patient could be categorized as either healed or not. One patient who had both two healed plaques and one residual ruptured plaque was excluded from the following analysis. The clinical characteristics at follow-up in patients with healed plaques (n = 10) and in those without healed plaques (n = 19) are summarized in Table 4. The frequency of statin use in patients with healed plaques was higher than that in those without healed plaques (p = 0.009). In patients with healed plaques, the serum CRP level did not change significantly from 0.24 ± 0.34 mg/dl at baseline to 0.07 ± 0.03 mg/dl at follow-up (p = 0.16). The serum CRP level in patients with healed plaque was lower than that in those without healed plaques (0.07 ± 0.03 mg/dl vs. 0.15 ± 0.11 mg/dl; p = 0.007).

The results of univariate logistic regression analyses indicated that the serum CRP level at follow-up and statin use were predictors for plaque healing in nonculprit lesions (Table 5). Multivariate logistic regression analysis was performed, in which the serum CRP level at follow-up and statin use were the independent variables. Two clinical variables were not statistically significant (serum CRP level at follow-up: p = 0.12, odds ratio 1.21, 95% confidence interval 0.99 to 1.62; statin use: p = 0.19, odds ratio 0.27, 95% confidence interval 0.04 to 1.83).

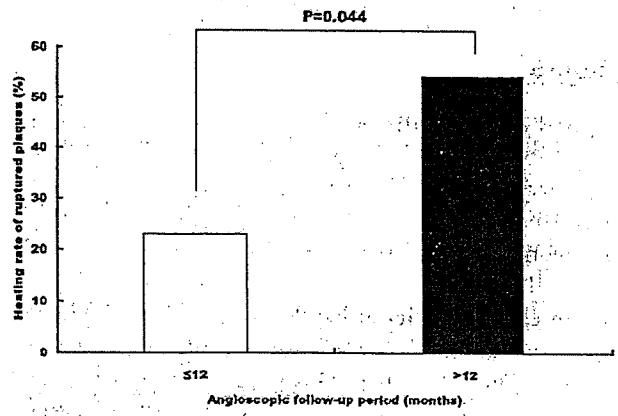

Figure 3. Relationship between the angioscopic follow-up period and healing rate of the nonculprit ruptured plaques. The healing rate of ruptured plaques of ≤12 months and >12 months were 23% and 55%, respectively. The healing rate increased according to the angioscopic follow-up period.

JACC Vol. 45, No. 5, 2005
March 1, 2005:652–8

Table 4. Patient Characteristics at Follow-Up

	Patients With Healed Plaques (n = 10)	Patients Without Healed Plaques (n = 19)	p Value
Serum LDL-C level (mg/dl)	109 ± 28	128 ± 31	0.13
Changes in serum LDL-C level (mg/dl)	−51 ± 50	−24 ± 37	0.15
Serum CRP level (mg/dl)	0.07 ± 0.03	0.15 ± 0.11	0.007
Medication			
Antiplatelet	10 (100%)	19 (100%)	>0.99
Warfarin	0	1 (5%)	0.46
Angiotensin-converting enzyme inhibitor	5 (50%)	6 (32%)	0.33
Angiotensin receptor blocker	3 (30%)	5 (26%)	0.83
Beta-blocker	2 (20%)	6 (32%)	0.51
Statin	7 (70%)	4 (21%)	0.009

Data are presented as the mean value ± SD or number (%) of patients. The Fisher exact test was used for categorical data. Abbreviations as in Table 1.

Clinical events. All patients underwent successful PCI for culprit lesions at baseline. The clinical follow-up period was 38 ± 16 months. Five patients underwent repeat PCI for restenosis at three to six months after baseline. A new onset of effort angina (SAP) occurred in one patient 25 months after baseline. In this patient, a healed plaque confirmed by angioscopy showed progression on an angiogram, and PCI was performed. All patients were free from bypass surgery, ACS, and death during the clinical follow-up period.

DISCUSSION

Multiple coronary plaque ruptures, including culprit plaque and other plaques, can occur in patients with various ischemic heart disease (6–10). At the present time, ruptured plaque in the culprit lesion is commonly treated by PCI. This follow-up study clarified the changes in ruptured plaques in nonculprit lesions.

Change of thrombus color and plaque healing. A previous IVUS study reported the frequencies of thrombus in nonculprit ruptured plaques in ACS and in non-ACS to be 32% and 8%, respectively (8). In this angioscopic study, 48 (96%) of 50 ruptured plaques were associated with superimposed thrombi. Coronary angioscopy might be superior to IVUS regarding its ability to differentiate plaque from thrombus. Moreover, angioscopy can show the thrombus color, which allows us to estimate the age and components of the thrombus. In this study, the predominant thrombus color changed from red at baseline to pinkish-white at follow-up. A red thrombus on angioscopy is considered to be a fresh one and is mainly composed of red blood cells and fibrin. In the process of thrombus organization, a red thrombus changes into a pinkish-white one with platelets and fibrin formation (3,16). Our observations on the changes in thrombus color might show the process of thrombus organization.

Table 5. Predictors for the Healing of Nonculprit Ruptured Plaques

	p Value	Odds Ratio	95% CI
Serum LDL-C level at follow-up	0.057	1.03	0.99–1.06
Changes in serum LDL-C level	0.151	1.01	1.00–1.04
Serum CRP level at follow-up	0.004	1.28	1.06–1.68
Statin use	0.010	0.11	0.02–0.60

CI = confidence interval; other abbreviations as in Table 1.

In our study, the angioscopic follow-up period varied. However, the frequency of disappearance of thrombus and healed plaque increased gradually according to the follow-up period. The frequency of yellow plaques in the healed plaques was lower than that at baseline. In several cases, the plaque color changed from yellow to white during the healing process. Similar to the healing of culprit plaques after PCI, a white neointima on angioscopy may cover the nonculprit ruptured plaques and also play a role in the repair process (17). Surprisingly, several thrombi were still found on the ruptured plaque after 12 months of follow-up. These results may suggest that ruptured plaques heal very slowly. A previous pathologic study demonstrated that repetitive ruptures occur in the healed plaques (10). Perhaps part of the thrombi form after recurrent ruptures, and repetitive ruptures could not be excluded in our study.

Change in angiographic stenosis. The %DS of the healed plaques increased significantly from baseline to follow-up. A postmortem study in patients with sudden cardiac death reported that the area within the internal elastic lamina is less in healed plaque after a subclinical rupture than in acute ruptured plaque (10). Furthermore, a cellular proliferation of smooth muscle cells is higher at healed plaque than at ruptured plaque (10). These facts suggest that plaque healing results in an increased plaque burden and negative remodeling.

Our past combination study using angioscopy and IVUS revealed that nondisrupted white plaque and negative remodeling are often found in the culprit lesions of SAP (18). Probably, in several cases of SAP, stenosis of the coronary lumens developed, and clinical symptoms have appeared in the process of plaque healing after previous ruptures. The precise mechanism of angiographic progression was not clarified in this angioscopic study, although progression of

the healed plaques might have resulted from negative remodeling and cell infiltration into the plaques.

Serum CRP level. The serum CRP level predicts the risk of MI or stroke better than total and low-density lipoprotein cholesterol levels (12). A previous angiographic study revealed the presence of multiple complex stenosis in ACS patients, and such stenosis was found to correlate with elevated CRP levels (19). In our study, the serum CRP level in patients with healed plaques did not significantly decrease from baseline to follow-up. The serum CRP level in patients with healed plaques was lower than that in those without healed plaques, thus suggesting that the serum CRP level should reflect the disease activity of the plaque ruptures.

Pharmacologic intervention with statin therapy has been shown to reduce the serum CRP level. We previously reported that statin therapy reduces the serum CRP level and angioscopic complexity of the plaques (the existence of the thrombus and the irregularity of the plaque) in nonculprit lesions (20). Our present data show that frequency of administration of a statin in patients with healed plaques was significantly higher than that in those without healed plaques. Moreover, the serum CRP level in patients with healed plaques was lower than that in those without healed plaques. Our results from univariate logistic regression analyses indicated that both statin therapy and serum CRP level at follow-up are considered predictors of healing in nonculprit ruptured plaques. However, a multivariate logistic regression analysis showed that neither statin therapy nor serum CRP level at follow-up is an independent predictor of plaque healing. These results should be explained so that these two factors correlate to each other.

Clinical events. In this study, no patients had any ACS events during the 38-month follow-up without PCI for nonculprit ruptured plaques. A previous angiographic study in ACS patients with complex coronary lesions demonstrated a poor clinical prognosis, particularly in terms of recurrent ACS episodes (21). On the other hand, an IVUS study of multiple coronary ruptures revealed no recurrence of ACS during 10-month clinical follow-up (6). In the same study, the stenosis of ruptured plaques in nonculprit lesions was less severe than that in culprit lesions (39% vs. 70%, respectively). In our study, the %DS was only 16.3% in ruptured plaques of baseline and 19.1% in nonhealed plaques of follow-up. A quantitative cross-sectional analysis by IVUS revealed that ruptured plaques at nonculprit lesions have larger lumens than do culprit lesions (6,8). Such evidence indicates that a plaque rupture itself does not always result in acute ischemic events. Our follow-up study suggests that even though there are residual ruptured plaques and thrombi, the associated lesions do not lead to the development of ACS in cases with large coronary lumens.

However, an important question remains. Angiographic studies have shown that preexisting stenoses of the culprit lesions were previously mild to moderate (22,23). It is impossible to explain that the degree of stenosis on the angiogram can help determine whether the patient develops ACS or the plaque ruptures remain asymptomatic. When patients have a systemic or local increased potential of thrombogenicity, ruptured plaques in lesions with mild to moderate stenosis may lead to ACS (24). Several IVUS studies have demonstrated that culprit lesions of ACS have a greater plaque burden than do ruptured plaques in nonculprit lesions (6–8). In the event of a plaque rupture, a large plaque is considered to contribute to accelerated local thrombogenicity and the development of thrombosis because of the exposure of a large amount of its contents, such as tissue factor and collagen (25). Conversely, at the nonculprit plaques in smaller sized plaques, even though thrombi still remain, growth of the thrombi may be limited. Therefore, both the degree of stenosis and plaque size, which are unable to be validated by an angiogram, may thus be determinant factors in the clinical course of ruptured plaques.

Atherosclerosis is a progressive disease. Repetitive coronary plaque ruptures on the healed plaques can occur, and then the degree of luminal narrowing should progress (10). A significant degree of stenosis thus appears to be associated with the cause acute thrombotic events (26). Further follow-up studies are needed to examine the development of severe stenosis and acute coronary events.

Study limitations. The number of analyzed plaques and patients represent a limitation of this study. Coronary angioscopy was not performed in all segments of coronary arteries in all patients. Some selection bias is therefore inevitable, beginning with the selection of patients to undergo cardiac catheterization and angioscopy. The follow-up angioscopic examination, which was performed at a single time point, also has some limitations.

Conclusions. This follow-up study documented that plaque ruptures in nonculprit lesions tend to heal slowly with a progression of luminal stenosis, and the serum CRP level might reflect the disease activity of the plaque ruptures.

Acknowledgments

The authors thank Koji Harada, Masayuki Mizuno, Yoshiko Kasahara, and Mizue Yoshitomi for their excellent assistance in our catheter laboratory. Finally, we thank Shinji Hirosaki for his statistical advice.

Reprint requests and correspondence: Dr. Kyoichi Mizuno, Department of Internal Medicine, Chiba-Hokusoh Hospital, Nippon Medical School, 1715 Kamakari, Imba, Chiba, Japan 270-1694. E-mail: mizunok@nms.ac.jp.

REFERENCES

1. Fuster V, Badimon L, Badimon JJ, et al. The pathogenesis of coronary artery disease and the acute coronary syndromes. N Engl J Med 1992;326:242–50, 310–8.
2. Mizuno K, Miyamoto A, Satomura K, et al. Angioscopic macromorphology in patients with acute coronary disorders. Lancet 1991;337: 809–12.

3. Mizuno K, Satomura K, Miyamoto A, et al. Angioscopic evaluation of coronary-artery thrombi in acute coronary syndromes. N Engl J Med 1992;326:287–91.
4. Falk E, Shah PK, Fuster V. Coronary plaque disruption. Circulation 1995;92:657–71.
5. Farb A, Burke AP, Tang A, et al. Coronary plaque erosion without rupture into a lipid core: a frequent cause of coronary thrombosis in sudden coronary death. Circulation 1996;93:1354–63.
6. Rioufol G, Finet G, Ginon I, et al. Multiple atherosclerotic plaque rupture in acute coronary syndrome: a three-vessel intravascular ultrasound study. Circulation 2002;106:804–8.
7. Kotani J, Mintz GS, Castagna T, et al. Intravascular ultrasound analysis of infarct-related and non-infarct-related arteries in patients who presented with an acute myocardial infarction. Circulation 2003; 107:2889–93.
8. Fujii K, Kobayashi Y, Mintz GS, et al. Intravascular ultrasound assessment of ulcerated ruptured plaques: a comparison of culprit and nonculprit lesions of patients with acute coronary syndromes and lesions in patients without acute coronary syndromes. Circulation 2003;108:2473–8.
9. Schoenhagen P, Stone GW, Nissen SE, et al. Coronary plaque morphology and frequency of ulceration distant from culprit lesions in patients with unstable and stable presentation. Atheroscler Thromb Vasc Biol 2003;23:1895–900.
10. Burke AP, Kolodgie FD, Farb A, et al. Healed plaque ruptures and sudden coronary death: evidence that subclinical rupture has a role in plaque progression. Circulation 2001;103:934–40.
11. Mann J, Davies MJ. Mechanisms of progression in native coronary artery disease: role of healed plaque disruption. Heart 1999;82:265–8.
12. Ridker PM, Rifai N, Rose L, et al. Comparison of C-reactive protein and low-density lipoprotein cholesterol levels in the prediction of first cardiovascular events. N Engl J Med 2002;347:1557–65.
13. Glass CK, Witztum JL. Atherosclerosis: the road ahead. Cell 2001; 104:503–16.
14. Vainas T, Lubbers T, Stassen FR, et al. Serum C-reactive protein level is associated with abdominal aortic aneurysm size and may be produced by aneurismal tissue. Circulation 2003;107:1103–5.
15. Okamatsu K, Takano M, Sakai S, et al. Elevated troponin T levels and lesion characteristics in non-ST-elevation acute coronary syndromes. Circulation 2004;109:465–70.
16. Pearson TA, Dillman J, Solez K, et al. Monoclonal characteristics of organizing arterial thrombi: significance in the origin and growth of human atherosclerotic plaques. Lancet 1979;1:7–11.
17. Sakai S, Mizuno K, Yokoyama S, et al. Morphologic changes in infarct-related plaque after coronary stent placement: a serial angioscopy study. J Am Coll Cardiol 2003;42:1558–65.
18. Takano M, Mizuno K, Okamatsu K, et al. Mechanical and structural characteristics of vulnerable plaques: analysis by coronary angioscopy and intravascular ultrasound. J Am Coll Cardiol 2001;38:99–104.
19. Zairis M, Papadaki O, Manousakis S, et al. Multiple complex coronary plaques in patients with primary unstable angina. Atherosclerosis 2000;164:355–9.
20. Takano M, Mizuno K, Yokoyama S, et al. Changes in coronary plaque color and morphology by lipid-lowering therapy with atorvastatin: serial evaluation by coronary angioscopy. J Am Coll Cardiol 2003;42: 680–6.
21. Goldstein JA, Demetriou D, Grines CL, et al. Multiple complex coronary plaques in patients with acute myocardial infarction. N Engl J Med 2000;343:915–20.
22. Little WC, Constantinescu M, Applegate RJ, et al. Can coronary angiography predict the site of a subsequent infarction in patients with mild-to-moderate coronary artery disease? Circulation 1988;78:1157–66.
23. Fishbein MC, Siegel RJ. How big are coronary atherosclerotic plaques that rupture? Circulation 1996;94:2662–6.
24. Naghavi M, Libby P, Falk E, et al. From vulnerable plaque to vulnerable patient: a call for new definitions and risk assessment strategies: part I. Circulation 2003;108:1664–72.
25. Barstad RM, Hamers MJ, Kierulf P, et al. Procoagulant human monocytes mediated tissue factor/factor VIIa-dependent platelet-thrombus formation when exposed to flowing nonanticoagulated human blood. Atheroscler Thromb Vasc Biol 1995;15:11–6.
26. Qiao JH, Fishbein MC. The severity of coronary atherosclerosis at sites of plaque rupture with occlusive thrombosis. J Am Coll Cardiol 1991;17:1138–42.